AIP | Applied Physics Letters

Compositional dependence of shear-band dynamics in the Zr–Cu–Al bulk metallic glass system

P. Thurnheer, R. Maaß, S. Pogatscher, and J. F. Löffler

Citation: Applied Physics Letters **104**, 101910 (2014); doi: 10.1063/1.4867240
View online: http://dx.doi.org/10.1063/1.4867240
View Table of Contents: http://scitation.aip.org/content/aip/journal/apl/104/10?ver=pdfcov
Published by the AIP Publishing

Compositional dependence of shear-band dynamics in the Zr–Cu–Al bulk metallic glass system

P. Thurnheer,[1] R. Maaß,[2,a)] S. Pogatscher,[1] and J. F. Löffler[1,b)]
[1]*Laboratory of Metal Physics and Technology, Department of Materials, ETH Zurich, 8093 Zurich, Switzerland*
[2]*Institute for Materials Physics, University of Göttingen, Friedrich-Hund Platz 1, 37077 Göttingen, Germany*

(Received 21 January 2014; accepted 18 February 2014; published online 13 March 2014)

Shear-band velocities of individual shear bands in $Zr_xCu_{90-x}Al_{10}$ ($x = 45$–65) metallic glasses were investigated as a function of temperature and Zr-content. The apparent activation energy of the shear-band propagation dynamics increases with Zr-content, giving evidence for the sensitivity of inhomogeneous plastic flow and related time scales to chemical composition. The shear-band viscosities derived display a Zr-content trend which contrasts with equilibrium viscosities in the supercooled liquid regime. These findings are discussed in terms of effective temperature and short-range order. © *2014 AIP Publishing LLC*. [http://dx.doi.org/10.1063/1.4867240]

Metallic glasses (MGs) are promising candidates for structural components. With a propensity for brittle failure, applications of MGs currently focus on elastic properties. However, depending on temperature and straining conditions, MGs can also be strained plastically by a considerable amount. They can exhibit large homogeneous ductility at temperatures around and beyond the glass transition temperature T_g.[1] For some alloys, stable plastic flow may also be observed in both tension and compression well below T_g.[2] Because runaway cracks are inhibited, plastic strain at failure in compression exceeds values obtained in tension by far and is therefore better suited for studying the dynamics of the underlying carriers of macroscopic plastic flow, i.e., nm-thin shear bands.[3–5]

Depending on temperature and strain rate, compressive flow curves are smooth (non-serrated) or discontinuous (serrated).[6] This is a direct result of the structural, atomistic dynamics in the activated shear band. Indeed, the transition between these two flow modes is known to be thermally activated,[7–9] a phenomenon which more recent investigations have linked to the thermally activated nature of shear-band propagation dynamics.[10] The temperature and rate-dependent transition between serrated and non-serrated flow was shown to reflect a competition between experimental time scales (applied strain rate) and structural relaxation kinetics.[9,11,12]

These new insights into shear-band dynamics rely on the fact that a specific serration can be directly linked to the operation of one shear band only. While this has been debated intensely,[13–15] our own efforts to trace the shear offset of a single shear band for consecutive serrations,[12] as well as state-of-the art high-speed camera studies by Wright *et al.*,[16] clearly demonstrate a 1:1 correlation. In addition, Wright and co-workers made a valuable contribution towards resolving the long-standing question of whether a shear band propagates via simultaneous motion across its entire shear plane, or rather via a propagation front mechanism.[16] Their high-speed imaging experiment revealed simultaneous sliding along the shear band, supporting previous work.[15,17] With this in mind, shear-band propagation velocities can be captured provided that a sufficiently high data sampling rate is used, to generate real-time information on shear-band dynamics.

Up to now our efforts have concentrated on temperature-dependent shear-band dynamics, targeting shear-band initiation,[18] propagation,[10,12] and arrest[11] of Vit105 ($Zr_{52.5}Cu_{17.9}Ni_{14.6}Al_{10}Ti_5$). In this study, we extend our efforts to compositional effects, with the aim of understanding and eventually controlling shear banding in MGs and therefore low-temperature malleability.

In this Letter, we report on shear-band dynamics measurements in the system $Zr_xCu_{90-x}Al_{10}$, with $x = 45$, 50, 55, 60, and 65. This system was chosen because of its proximity to Vit105, with the additional benefit of detailed knowledge on compositionally related changes in local structure provided by molecular dynamics simulations.[19]

For the $Zr_xCu_{90-x}Al_{10}$ ($x = 45$–65) MG production, high-purity pre-alloys (raw material purity: Zr-99.9%, Cu-99.995%, Al-99.999%) were prepared in an arc-melting furnace. Ten cycles of re-melting and flipping were performed to ensure the best possible chemical homogeneity. Rods of 2 mm in diameter were obtained by suction casting. The glassy material was subsequently shown to be amorphous using X-ray diffraction and to have a glass transition in differential scanning calorimetry (DSC, not displayed here). As shown elsewhere, the glass transition of the MGs decreases with increasing Zr-content.[20] Compression specimens with a length of 4 mm were cut from the rods. The top and bottom surfaces of each sample were made plane-parallel via grinding and polishing. Following the procedure outlined in Ref. 21, the samples were notched (depth 150 μm, orientation 45°) via electric discharge machining with a 100 μm thin copper wire, in order to avoid shear-band initiation at contact points of the sample with the cross-head platens of the testing machine, which would generate constrained shear-band dynamics. Thus the data displayed in the following represent constraint-free major shear banding in the absence of geometrical arrest. Temperature-dependent (200 K–320 K) compression tests were

a)Electronic mail: robert.maass@ingenieur.de.
b)Electronic mail: joerg.loeffler@mat.ethz.ch.

conducted at a strain rate of $10^{-4}\,s^{-1}$ to $10^{-3}\,s^{-1}$ and a data sampling rate of 5 kHz. Further details of the experimental setup are found in Ref. 12. For each serration occurring, we derived the shear-band velocity, v_{SB}, according to[12]

$$v_{SB} = \sqrt{2}\frac{\Delta u_{pl}}{\Delta t} = \sqrt{2}\frac{\Delta u_0 + \Delta F C_s}{\Delta t}, \quad (1)$$

where Δu_{pl} is the true plastic displacement and Δt is the duration of a single slip event. The pre-factor accounts for the shear-band angle of approximately 45° relative to the loading axis. The term Δu_{pl} is expressed as the sum of the measured displacement jump Δu_0 and a correction factor, given by the product of load drop ΔF and sample compliance C_s, which accounts for the amount of elastic displacement that is converted into plastic displacement during the instability.

Figure 1(a) shows the engineering stress-strain curves for the compositions studied at 243 K. It is notable that the data in Fig. 1(a) exhibit no apparent strain hardening or constant flow-stress plateau. Indeed, all curves show pronounced strain softening, which we attribute to the geometrically unhindered propagation of a major shear band initiated at the notch. Further, the strength σ_y decreases with increasing Zr-content, following the same trend as the glass transition temperature. This is in general agreement with the existence of a universal yield criterion in metallic glasses.[22] As an example, the inset to Fig. 1(a) displays a stress-time trace for a series of serrations in $Zr_{65}Cu_{25}Al_{10}$, indicating a very regular spacing that is observed across all compositions. In Fig. 1(b) the shear-band velocities, derived from the same curves as presented in Fig. 1(a), are depicted as a function of plastic engineering strain. We define plastic engineering strain to be zero where the maximum stress is reached, which coincides well with the elastic-plastic transition. The shear-band velocity as a function of plastic strain shows a semi-circular behavior, spanning almost one order of magnitude in v_{SB}. Due to limited malleability, this velocity-strain scaling is not observed for $Zr_{45}Cu_{45}Al_{10}$ at 243 K. At this stage it is clear that both a strain and compositional dependence of v_{SB} is found. The non-monotonic trend of v_{SB} as a function of Zr-content cannot be straightforwardly characterized with a single parameter. We have thus explored five different methodologies, which are (i) an average velocity from 0 to 0.25% plastic strain, termed $v_{SB\text{-}1}$, (ii) an average velocity from 1 to 1.5% plastic strain, called $v_{SB\text{-}2}$, (iii) an average velocity of all values centered symmetrically (±0.25%) around the maximum shear-band velocity, termed $v_{SB\text{-}max}$, (iv) averaging all values from zero plastic strain to the maximum shear-band velocity, called $v_{SB\text{-}mean}$, and finally (v) the slope of a linear fit of the increasing regime up to the maximum velocity (v_{fit}).

Figure 2 summarizes the calculated shear-band velocities (at 243 K) for all five approaches taken and demonstrates the robustness of the analysis method: irrespective of the strain regime, the shear-band velocity decreases with increasing Zr-content. The same trend is observed for v_{fit}. In the following we focus our analysis on $v_{SB\text{-}1}$, motivated by the ability to also capture the dynamics of the Zr-poor alloy ($x = 45$).

As a next step, the temperature-dependent shear-band velocity for all alloy compositions was investigated. Figure 3(a) plots $v_{SB\text{-}1}$ as a function of the Zr-content for $T = 223$, 243, 263, and 283 K. For all temperatures studied, the shear-band propagation velocity decreases with increasing Zr-content. Note that for $x = 45$ and 50 a ductile-to-brittle transition is observed at about 243 K, and therefore $v_{SB\text{-}1}$ could not be evaluated at larger T. Such ductile-to-brittle transitions below T_g have already been reported for Vit105 (Ref. 9) and for a series of Au-based metallic glasses.[23] The temperature-dependent shear-band velocity can now be converted into shear-band viscosities (Fig. 3(b), as an example for $T = 243$ K) via[24]

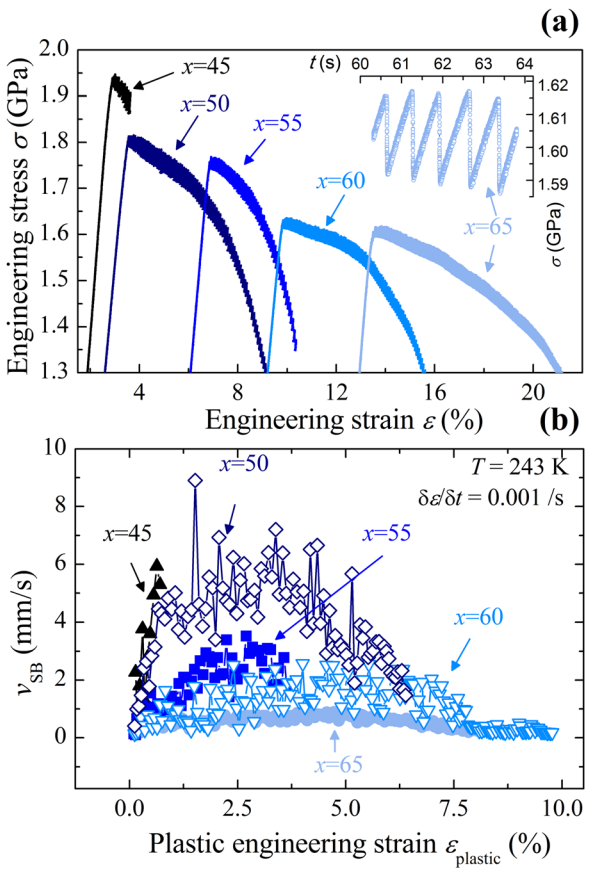

FIG. 1. (a) Flow curves for $Zr_xCu_{90-x}Al_{10}$ at 243 K. The inset shows a close-up of the serrated flow regime for the alloy with $x = 65$. (b) Shear-band velocities obtained from the flow curves in (a) as a function of plastic engineering strain $\varepsilon_{plastic}$.

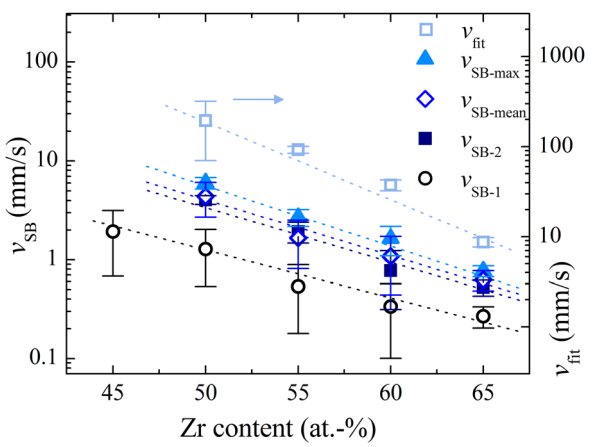

FIG. 2. Compositionally dependent shear-band dynamics at 243 K, assessed according to five different one-parameter description methods. Lines are guides for the eye.

$$\eta_{SB} = \frac{\tau w}{v_{SB}}, \quad (2)$$

where τ is the shear stress, i.e., $\sigma_y/2.01$, and w is the shear-band thickness, here taken as 10 nm.[3,25,26] We have seen that with increasing Zr-content, τ (or σ_y) decreases (Fig. 1). The decrease in this direct stress term over the tested compositions is, however, small compared to the pronounced decrease in v_{SB}. The result of Eq. (2) is thus a shear-band viscosity which increases with increasing Zr-content (Fig. 3(b)).

In agreement with our earlier work,[10,12] it is found that the shear-band velocity obeys an apparent Arrhenius behavior for all alloys. Figure 4 displays $v_{SB\text{-}1}$ as a function of $1/T$, where the shear-band velocities cover three orders of magnitude ranging from 0.01 to 10 mm/s over the temperature regime tested. The experimental data are fit with an Arrhenius-type function, for which the resulting lines are also shown in Fig. 4. We note that the trend in Fig. 4 is true for any of the five parameters presented in Fig. 2. Table I summarizes the apparent activation energy, $Q_{SB\text{-}1}$, obtained from $v_{SB\text{-}1}$, and an average value, $\bar{Q}$, obtained by averaging the apparent activation energies of all evaluation methods. The standard deviation, $\bar{\sigma}$, and the mean fitting error, $\bar{\Delta}$, for $\bar{Q}$ are also given.

Due to the limited ductility of the $Zr_{45}Cu_{45}Al_{10}$ alloy only $v_{SB\text{-}1}$ was used to analyze $\bar{Q}$ for that composition. We find that the activation energy ranges from 0.28 to 0.35 eV. Over the entire range of Zr-content, a slight increase in the activation energy is seen, predominantly manifested by $x = 60$ and $x = 65$. For comparison Table I also includes the apparent activation energy for shear-band propagation velocities derived for Vit105.[10,12]

The experimental data outlined above thus demonstrate a slowdown of the shear-band dynamics, i.e., an increasing barrier against sliding, of $Zr_xCu_{90-x}Al_{10}$ MGs with increasing

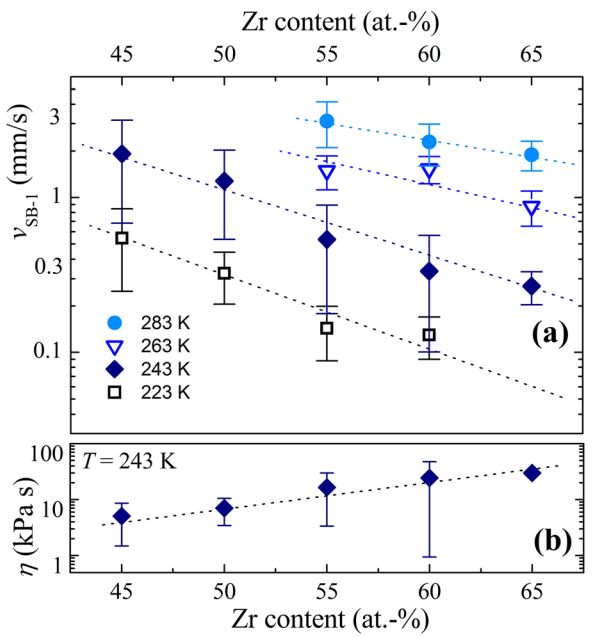

FIG. 3. (a) Shear-band velocity $v_{SB\text{-}1}$ at different temperatures as a function of the Zr-content. (b) Shear-band viscosity at 243 K as a function of the Zr-content. Lines are guides for the eye.

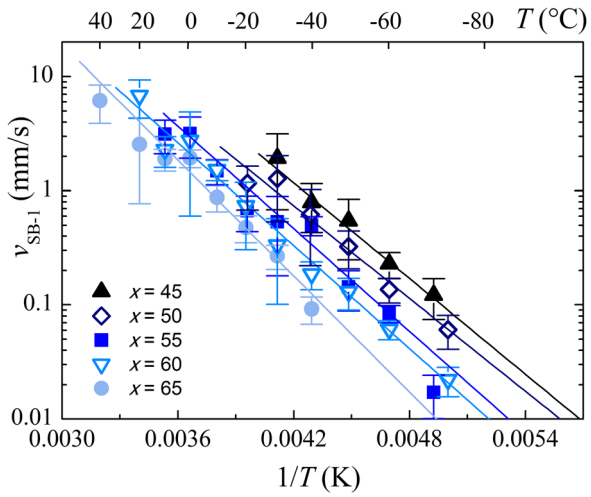

FIG. 4. Arrhenius representation of the temperature dependence of $v_{SB\text{-}1}$. Lines are fits using a simple Arrhenius-type function.

Zr-content. Before searching for the origin of this compositional trend, it is instructive to investigate which of the factors in Eq. (1) are responsible for the slowdown in kinetics with increasing Zr-content at a given temperature. The data acquired reveal that the dominating effect arises from an increase of approximately one order of magnitude in Δt with an increasing amount of Zr (not shown) whereas the slip-size magnitudes remain similar within a factor of 2; a degree of scatter that is difficult to separate from the spread within a single test. Based on this and on the fact that a velocity profile during a stress drop has a symmetric profile,[11] we can conclude that $\Delta t = \tau_{acceleration} + \tau_{deceleration} \sim x$, i.e., the atomistic time scales of the underlying processes increase with an increasing amount of Zr, under the assumption that shear-band acceleration and deceleration contribute equally. Consistent with the increase of $Q_{SB\text{-}1}$ and $\bar{Q}$ as a function of Zr-content, it is found that the shear-band velocity decreases and the transient viscosity according to Eq. (2) increases.

Since shear softening in conjunction with shear-band initiation is viewed as a mechanically induced glass transition,[27] which can be described by a rise in the material's effective temperature,[28,29] it seems natural to compare shear-band viscosities to equilibrium viscosities obtained directly in the supercooled liquid regime. In so doing, we find that the equilibrium viscosities[30] follow a compositional trend opposite to the one displayed in Fig. 3(b): equilibrium viscosities are lowest for Zr-rich alloys. Clearly, absolute viscosity values should not be directly compared because the shear-band

TABLE I. Apparent activation energy $Q_{SB\text{-}1}$, average activation energy $\bar{Q}$, standard deviation $\bar{\sigma}$, and averaged fitting error $\bar{\Delta}$ as a function of the Zr-content x. The data for Vit105 were obtained from Refs. 10 and 12.

x (at. %)	$Q_{SB\text{-}1}$ (eV)	$\bar{Q}$ (eV)	$\bar{\sigma}$ (eV)	$\bar{\Delta}$ (eV)
45	**0.28 ± 0.09**	**0.28**	…	0.09
50	**0.26 ± 0.05**	**0.29**	0.03	0.03
55	**0.30 ± 0.03**	**0.28**	0.02	0.02
60	**0.30 ± 0.02**	**0.32**	0.02	0.03
65	**0.35 ± 0.04**	**0.35**	0.01	0.03
Vit105		**0.32**	…	0.01

viscosity describes a transient, nanoscopically confined state. However, if the effective temperature rise upon yielding was the same for all alloys, one would expect that the mere compositional trend of shear-band viscosity would be identical to that found in equilibrium. Our measurements show that this is not the case, pointing to an effective temperature rise ΔT_e that is indeed composition-dependent, meaning that shear bands in Zr-poor alloys undergo a larger effective temperature rise. One of the reasons for this may be the higher yield stress level at lower Zr-content (which must be considered as the driving force for a mechanically induced glass transition), but also to some extent the different changes in the short-range atomic structure.

While it is difficult to directly assess the atomic structure within an active shear band, atomistic modelling provides a conclusion which is qualitatively similar to that of the effective temperature. Molecular dynamics simulations of a Zr–Cu–Al MG have been shown to contain a distinctly occurring short-range order in the form of icosahedra.[19] These studies by Cheng *et al*. provided evidence that the fraction of icosahedra in $Cu_{46}Zr_{54}$ increases upon substitution of Zr by Cu or Al. Based on this, it can be argued that in our study a larger fraction of atoms is contained in icosahedra in the Zr-poor alloys. Upon yielding, it has been shown that the backbone of the icosahedra breaks,[31] which consequently leads to a reduction in flow resistance, here either expressed by the apparent viscosity (Fig. 3(b)) or the activation energies in Table I. This effect is more pronounced for the Zr-poor alloys studied, and thus provides a qualitative understanding, in good agreement with the trends displayed in Figs. 3(b) and 4.

In summary, we have investigated the compositional dependence of shear-band propagation velocities of a single shear band in the ternary Zr–Cu–Al MG system. Faster and less viscous shear dynamics characterize Zr-poor systems. All the alloys studied exhibit thermally activated shear-band dynamics with apparent activation energies that increase slightly with increasing Zr-content. This and the millisecond time scales measured for shear-band propagation clearly show that the shear-induced softening is due to dilatation rather than local adiabatic heating. The shear-band velocity also shows a clear dependence on plastic strain, which is found to have a negligible effect on the activation energy. The higher resistance to shear-band propagation in Zr-rich alloys can be understood by taking into account a lower effective temperature jump upon yielding of Zr-rich alloys. This also concurs with recent molecular dynamics simulations that ascribe a reduced flow resistance to Zr-poor alloys on the basis of breaking icosahedral short-range order.

The authors gratefully acknowledge funding by the Swiss National Science Foundation (SNF Grant No. 200020-135100) and thank A. Saeed-Akbari and D. Granata for fruitful discussions.

[1]Y. Kawamura, T. Nakamura, and A. Inoue, Scr. Mater. **39**, 301 (1998).
[2]C. A. Schuh, T. C. Hufnagel, and U. Ramamurty, Acta Mater. **55**, 4067 (2007).
[3]T. Masumoto and R. Maddin, Acta Metall. **19**, 725 (1971).
[4]D. Klaumünzer, R. Maaß, and J. F. Löffler, J. Mater. Res. **26**, 1453 (2011).
[5]A. L. Greer, Y. Q. Cheng, and E. Ma, Mater. Sci. Eng. R: Rep. **74**, 71 (2013).
[6]C. A. Pampillo and H. S. Chen, Mater. Sci. Eng. **13**, 181 (1974).
[7]H. Kimura and T. Masumoto, Philos. Mag. A **44**, 1021 (1981).
[8]A. Dubach, F. H. Dalla Torre, and J. F. Löffler, Philos. Mag. Lett. **87**, 695 (2007).
[9]A. Dubach, F. H. Dalla Torre, and J. F. Löffler, Acta Mater. **57**, 881 (2009).
[10]D. Klaumünzer, R. Maaß, F. H. Dalla Torre, and J. F. Löffler, Appl. Phys. Lett. **96**, 061901 (2010).
[11]R. Maaß, D. Klaumünzer, G. Villard, P. M. Derlet, and J. F. Löffler, Appl. Phys. Lett. **100**, 071904 (2012).
[12]R. Maaß, D. Klaumünzer, and J. F. Löffler, Acta Mater. **59**, 3205 (2011).
[13]B. E. Schuster, Q. Wei, T. C. Hufnagel, and K. T. Ramesh, Acta Mater. **56**, 5091 (2008).
[14]Y. H. Liu, C. T. Liu, A. Gali, A. Inoue, and M. W. Chen, Intermetallics **18**, 1455 (2010).
[15]S.-H. Joo, H. Kato, K. Gangwar, S. Lee, and H. S. Kim, Intermetallics **32**, 21 (2013).
[16]W. J. Wright, R. R. Byer, and X. Gu, Appl. Phys. Lett. **102**, 241920 (2013).
[17]S. X. Song, X. L. Wang, and T. G. Nieh, Scr. Mater. **62**, 847 (2010).
[18]D. Klaumünzer, A. Lazarev, R. Maaß, F. H. Dalla Torre, A. Vinogradov, and J. F. Löffler, Phys. Rev. Lett. **107**, 185502 (2011).
[19]Y. Q. Cheng, A. J. Cao, H. W. Sheng, and E. Ma, Acta Mater. **56**, 5263 (2008).
[20]Y. Yokoyama, K. Fukaura, and A. Inoue, Mater. Sci. Eng. A **375–377**, 427 (2004).
[21]R. Maaß, D. Klaumünzer, E. I. Preiß, P. M. Derlet, and J. F. Löffler, Scr. Mater. **66**, 231 (2012).
[22]W. L. Johnson and K. Samwer, Phys. Rev. Lett. **95**, 195501 (2005).
[23]D. Pan, H. Guo, W. Zhang, A. Inoue, and M. W. Chen, Appl. Phys. Lett. **99**, 241907 (2011).
[24]F. H. Dalla Torre, D. Klaumünzer, R. Maaß, and J. F. Löffler, Acta Mater. **58**, 3742 (2010).
[25]P. E. Donovan and W. M. Stobbs, Acta Metall. **29**, 1419 (1981).
[26]Y. Zhang and A. L. Greer, Appl. Phys. Lett. **89**, 071907 (2006).
[27]P. F. Guan, M. W. Chen, and T. Egami, Phys. Rev. Lett. **104**, 205701 (2010).
[28]M. L. Manning, E. G. Daub, J. S. Langer, and J. M. Carlson, Phys. Rev. E **79**, 016110 (2009).
[29]E. G. Daub, D. Klaumünzer, and J. F. Löffler, "Effective temperature dynamics of shear bands in metallic glasses," Phys. Rev. B (submitted).
[30]M. Yamada, Y. Tanimoto, T. Yamasaki, T. Kikuchi, Y. Yokoyama, and A. Inoue, J. Soc. Mater. Sci. Jpn. **59**, 124 (2010).
[31]A. J. Cao, Y. Q. Cheng, and E. Ma, Acta Mater. **57**, 5146 (2009).